

## Zoom Lens Design for a 10x Slim Camera using Successive Procedures

Sung-Chan Park<sup>1\*</sup> and Sang-Hun Lee<sup>2</sup>

<sup>1</sup>*Department of Physics, Dankook University, Cheonan 330-714, Korea*

<sup>2</sup>*LG Innotek Components R&D Center, LG Innotek, Ansan 426-791, Korea*

(Received October 29, 2013 : accepted November 11, 2013)

This study presents a new design method for a zoom lens, in which real lens groups are designed successively to combine to form a lens modules zoom system. The lens modules and aberrations are applied to the initial design for a four-group inner-focus zoom system. An initial design with a focal length range of 4.2 to 39.9 mm is derived by assigning the first-order quantities and third-order aberrations to each module along with the constraints required for optimum solutions. After obtaining the lens module zoom system, the real lens groups are successively, not separately, designed to get a zoom lens system. Compared to the separately designed real lens groups, this approach can give a better starting zoom lens and save time. The successively designed groups result in a zoom system that satisfies the basic properties of the zoom system consisting of the original lens modules. In order to have a slim system, we directly inserted the right-angle prism in front of the first group. This configuration resulted in a compact zoom system with a depth of 12 mm. The finally designed zoom lens has an f-number of 3.5 to 4.5 and is expected to fulfill the requirements for a mobile zoom camera having high zoom ratio of 10x.

**Keywords :** Lens module, Wave aberrations, Zoom lens, Optimization design

**OCIS codes :** (220.0220) Optical design and fabrication; (120.3620) Lens system design; (230.0230) Optical devices

### I. INTRODUCTION

The common zoom system is a multiple conjugates system allowing objects to be imaged on an image sensor with different scales. Designing a zoom lens consists of finding out the coupled motions of lens elements to accomplish the continuous variations of magnification or focal length. During the zooming, only the separations between elements vary at each zoom position. These separations are designated as an adjustment for changing magnifications and maintaining the image in focus.

Initial design methods for zoom lenses are usually divided into two ways. One is the paraxial analysis based on thin lens theory. The other is the optimized solution from lens modules design. The paraxial analysis has several disadvantages. It is difficult to judge if the solutions satisfy all the requirements for the zoom system [1-5]. Contrary to the paraxial method, since the lens module method employed in this study involves lots of physical quantities of the optical system, the first-order and third-

order aberrations can be manipulated directly by using lens modules [6-7]. Several zoom lenses have been designed and evaluated by lens modules [8-12].

In the previous design using lens modules, the real lenses for all groups are separately designed to match the first-order quantities and aberrations of the modules. And the separately designed groups are then combined to form an actual zoom lens. In this combining process, however, the stop position of each group is changed, which generates the large off-axis aberrations due to stop shift effects [13-15]. In our work, after obtaining the lens module zoom system, the real lens groups are successively, not separately, designed to get a zoom lens system. Compared to the previous design methods [8-12], this approach can give a better starting zoom lens, and save time and effort.

In this paper, lens modules and aberration theory are used to discuss the optimum initial design of a 10x, four-group inner-focus zoom system. This initial zoom system is designed to satisfy specific requirements, and the real lenses are successively obtained from the lens modules

\*Corresponding author: [scspark@dankook.ac.kr](mailto:scspark@dankook.ac.kr)

by using an automatic design method. In order to fold the ray path, the design reported recently has the minus-power single lens and a prism [16]. In this research, however, the right-angle prism was directly inserted without any lens in front of the first group. This configuration resulted in a much slimmer zoom system than the conventional system. After balancing of the higher-order aberrations, we obtained the zoom system that has the aperture of F/3.5 at position 1 to F/4.5 at position 3 and zoom ratio of 10x.

## II. LENS MODULE ZOOM SYSTEM DESIGN

Figure 1 illustrates the four-group inner-focus zoom system. From the object to the image side, the zoom system is composed of a fixed front group, a second lens group for zooming, a fixed third lens group, and a fourth lens group for focusing. Their powers are denoted  $k_1$ ,  $k_2$ ,  $k_3$ , and  $k_4$ , respectively. The distances between the preceding group and the succeeding group are denoted by  $d_{ij}$  ( $j=1, 2, 3, 4$ ) at  $i$ -th zoom position. The first and the third groups are always fixed. While the second group moves to the right to have a longer focal length, the fourth group should move to keep the image position stationary.

Each group is generally composed of several thick lens elements. When the higher-order aberrations are neglected, the properties of the lens system can be specified by its first-order quantities and the third-order wave aberrations at given conjugate points. In other words, if the first-order quantities and the third-order aberrations of the lens module are assigned to the real lens group, then both lens systems are equivalent to each other to within the limit of the first-and the third-order properties. Hence, each group of the zoom system can be replaced by its thick lens module by specifying its focal length( $FL_M$ ), front focal length( $FF_M$ ), back focal length( $BF_M$ ), magnification( $MG_M$ ), entrance pupil position( $EP_M$ ), entrance pupil diameter( $ED_M$ ), field angle( $\beta$ ), and third-order aberrations [13, 17].

We have set up the zoom lens system with four thick-lens modules, for which initial first-order inputs are

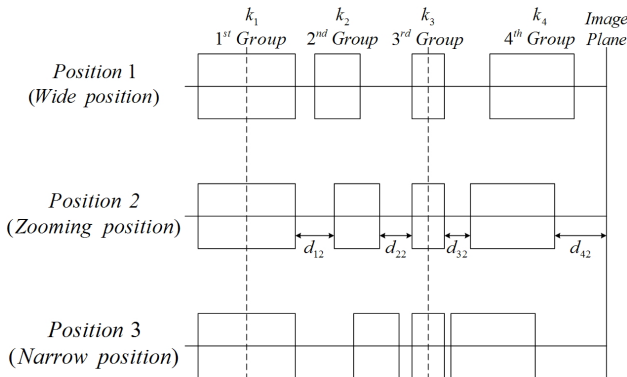


FIG. 1. Layout of the four-group inner-focus zoom system.

appropriately given to work as a zoom system. For the inner-focus zoom lens having high zoom ratio of 10x, the powers of the groups are generally composed such that the first, the third, and the fourth groups have positive powers, but the second group has a strong negative one. The aperture stop of the system is located in front of the third module so that the system has a symmetrical configuration with respect to the stop for aberration balancing. And then we reduced the aperture and image size of the initial zoom system so that the third-order aberrations were dominant. We have taken the zoom system with a half-image size of 1 mm and f-numbers of F/5 at position 1 to F/7 at position 3.

In order to get an optimum zoom system, the lens module prescriptions are optimized so that the specific constraints are satisfied. The specified constraints are the overall length of system, the equal distances between the first surface and stop at all zoom positions, focal lengths of 4.2 mm at position 1 to 39.9 mm at position 3, and good imagery. The constraint on the overall length should be as short as possible to reduce the system size. The design variables of each module are the focal lengths, the front focal lengths, the back focal lengths, the conjugate

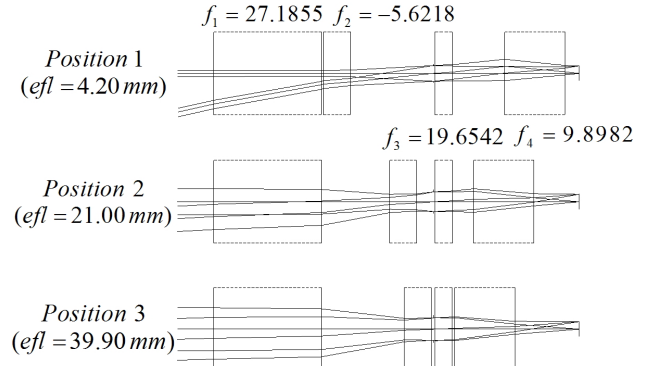


FIG. 2. Optimized zoom system consisting of four lens modules.

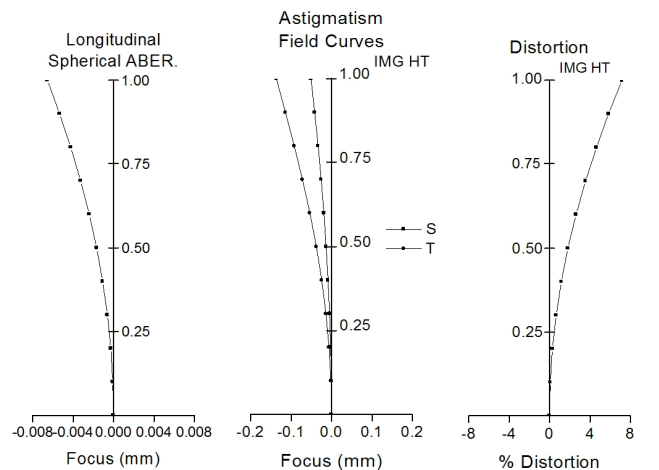


FIG. 3. The aberrations of the optimized lens module zoom system at position 1.

TABLE 1. Design data (in mm) for the lens modules in the optimized lens module zoom system

	Module I	Module II	Module III	Module IV
FL <sub>M</sub>	27.1855	-5.6218	19.6542	9.8982
FF <sub>M</sub>	-20.5173	6.6488	-20.9492	-15.4382
BF <sub>M</sub>	25.1694	-7.0725	16.8808	2.0409
MG <sub>M</sub>	0	-0.0256	0.0330	-0.0087
Thickness	15.6317	3.8945	2.5660	8.7709
W <sub>040</sub>	-0.0002	-0.3577	0.0091	-0.0098
W <sub>131</sub>	0.0054	0.2449	-0.0072	0.0136
W <sub>222</sub>	0.0025	-0.0422	0.0068	-0.0044
W <sub>220</sub>	-0.0047	0.0053	-0.0020	0.0000
W <sub>311</sub>	0.0017	-0.0175	0.0005	0.0039

TABLE 2. First-order properties and zooming locus of the optimized lens module zoom system consisting of four lens modules (in mm)

	Position1	Position2	Position3
efl	4.2000	21.0001	39.9005
bfl	2.0181	6.5603	9.3284
ffl	15.5669	9.2308	-61.0817
d <sub>1i</sub>	0.3000	9.9074	11.9973
d <sub>2i</sub>	12.0324	2.4249	0.3350
d <sub>3i</sub>	7.5953	3.0525	0.3000
d <sub>4i</sub>	2.0181	6.5602	9.3284

points, the spaces, and the aberration coefficients.

Figure 2 shows the optimum zoom system obtained from this process. It has a focal length of 4.2 to 39.9 mm, and the aberrations are corrected well, as shown in Fig. 3. Table 1 lists the design data of each module, and Table 2 gives the first-order properties and zooming locus at three positions. In Table 1, the values of  $W_{040}$ ,  $W_{131}$ ,  $W_{222}$ ,  $W_{220}$ , and  $W_{311}$  denote the third-order wave aberrations calculated at the edge of the field and the exit pupil in units of waves at the  $d$ -line [17]. Therefore, they correspond to the wave aberrations coefficients for spherical aberration, coma, astigmatism, Petzval curve, and distortion, respectively. In Table 2, the subscripts  $i$  denote zoom positions for zooming.

### III. CONVERTING LENS MODULES INTO REAL LENS GROUPS SUCCESSIVELY

The conversion of the lens module into a real lens group is based on the first-order and third-order aberration properties. To calculate aberrations of each group, we must know the aberration coefficients of each group, entrance pupil diameter, reference wavelength, and Lagrangian

invariant. The aberrations of each module are calculated at given f-number and wavelength of d-line by the Eqs. (1)~(6). In these equations, SA is spherical aberration, TCO is tangential coma, TAS is tangential astigmatism, SAS is sagittal astigmatism, PTB is Petzval blur, and DST is distortion [13, 17].

$$SA = -8\lambda_d Fno W_{040} \quad (1)$$

$$TCO = -6\lambda_d Fno W_{131} \quad (2)$$

$$TAS = -4\lambda_d Fno (W_{222} + W_{220}) \quad (3)$$

$$SAS = -4\lambda_d Fno W_{220} \quad (4)$$

$$PTB = -2\lambda_d Fno (2W_{220} - W_{222}) \quad (5)$$

$$DST = -2\lambda_d Fno W_{311} \quad (6)$$

If we separately convert the lens modules to real lens groups and then combine them to establish an actual zoom system, as in previous works [8-11], the position of the aperture stop at each group is changed. As a result, aberrations of each group are changed except spherical aberration and Petzval curvature. In this case, we must consider the stop shift effect in calculating the aberrations, however, it is very complex [13-15]. To avoid this difficulty, we successively converted lens modules to real lens groups.

In this paper, we used an optimization method so that the real lens equivalent to the module is obtained for each group. We choose appropriate structure for the real lens group and scaled up or down so that the focal length of each real lens group is the same as that of the lens module. And using the optimization method of Code-V, we matched the first-order quantities and third-order aberrations of the lens module to those of real lens. For the converting process, the design variables of the real lens are the radius of each surface, thickness and air space between the elements, and refractive index. The constraints are composed of the four first-order quantities of each module given in Table 1 and third-order aberrations calculated by Eqs. (1)~(6).

Figure 4 represents the converting process to the real lens of the first group only. Fig. 5 represents the aberrations of the system shown in Fig. 4 at position 1. At this time, other three groups are lens modules and, unlike the first group, have not been carried through the converting process. By these iterative processes, the second group, third group, and fourth group are successively converted to real lens groups. As a result, the lens module zoom system is group by group converted to the initial real lens zoom system without calculating the stop shift effect. Figure 6 represents the converting process to real lenses of the first and second groups, and Fig. 7 is the aberration of this system at position 1. Figure 8 represents converting process to real lenses of the first, second, and third groups. Figure 9 is the aberrations of the system shown in Fig. 8 at

position 1. Figure 10 represents the converting process to real lenses of all groups, and Fig. 11 is the aberrations of this system at position 1. By this converting process, we have easily obtained the four real lens groups reflecting the first-order quantities and third-order aberrations of lens modules.

Figure 12 represents the initial real lens zoom system combined due to zooming the locus listed in Table 2. As compared Fig. 3 to Fig. 11, the differences in aberration amount between the initial real lens system and the lens module system are caused by residual aberrations which are not considered in this section. These residual aberrations can be balanced by the optimization process. However, both lens systems have very similar aberration properties. Table 3 shows the first-order quantities and zooming locus of an initial real lens zoom system. From Table 2 and Table 3, the agreement for the first-order properties between both zoom systems is complete. This design procedure results in a real lens zoom system equivalent to the lens module zoom system, as shown in Fig. 12.

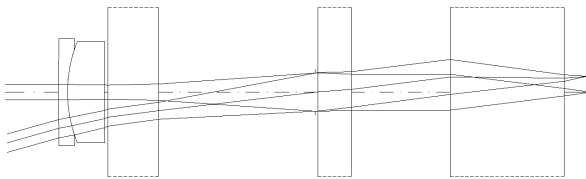


FIG. 4. The zoom system composed of a converted first real lens group and three modules at position 1.

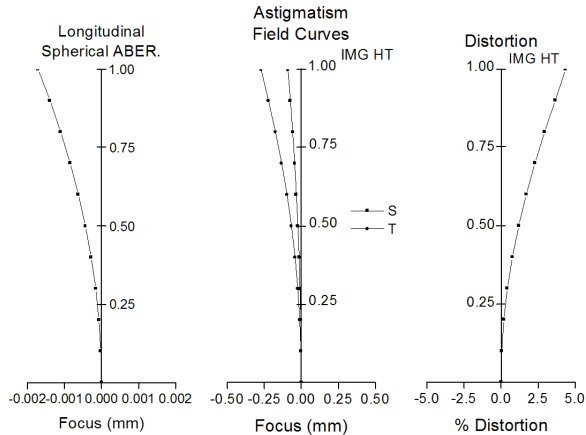


FIG. 5. The aberrations of the zoom system shown in Fig. 4.

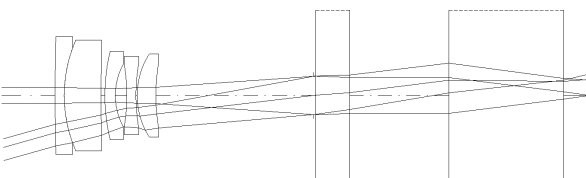


FIG. 6. The zoom system composed of the converted first, second real lens groups, and two modules at position 1.

#### IV. OPTIMIZED DESIGN FOR A SLIM ZOOM SYSTEM

Returning to the zoom system in Fig. 12, a glass block

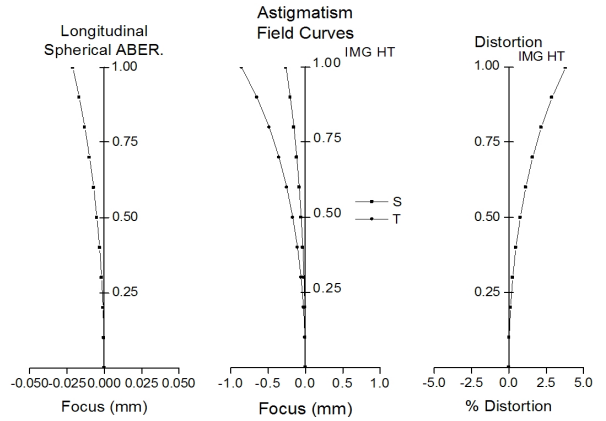


FIG. 7. The aberrations of the zoom system shown in Fig. 6.

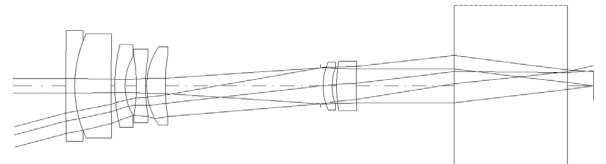


FIG. 8. The zoom system composed of the converted first, second, third real lens groups, and one module at position 1.

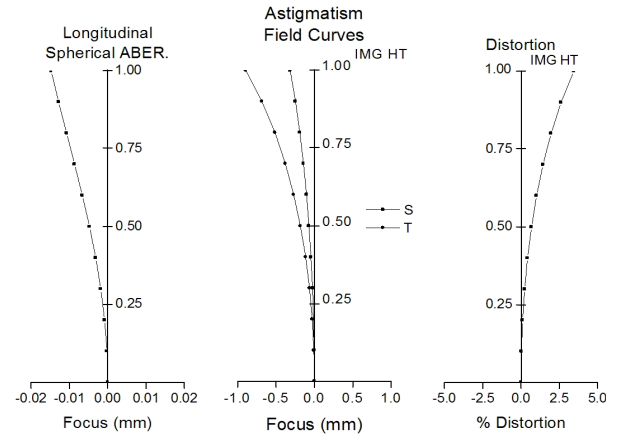


FIG. 9. The aberrations of the zoom system shown in Fig. 8.

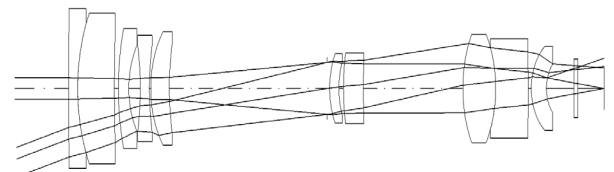


FIG. 10. The zoom system composed of all real lens groups at position 1.

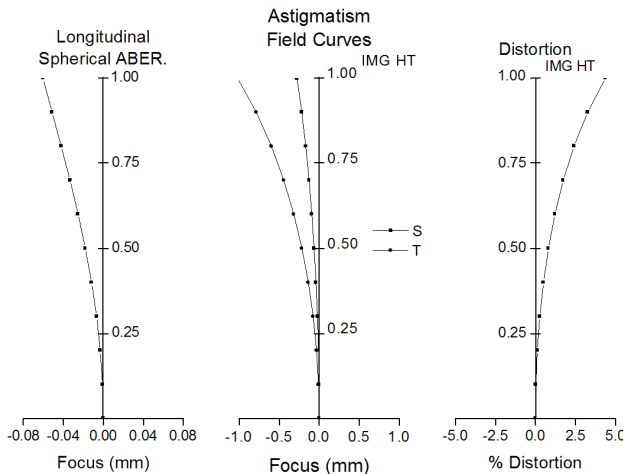


FIG. 11. The aberrations of the zoom system composed of all real lens groups shown in Fig. 10.

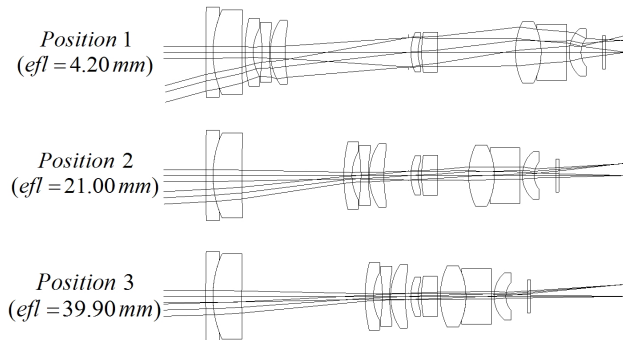


FIG. 12. Layout of an initial real lens zoom system.

TABLE 3. First-order properties and zooming locus of an initial real zoom system (in mm)

	Position1	Position2	Position3
$efl$	4.2000	21.0003	39.9013
$bfl$	2.0182	6.5604	9.3288
$ffl$	15.5669	9.2298	-61.0841
$d_{1i}$	0.3000	9.9074	11.9973
$d_{2i}$	12.0324	2.4249	0.3350
$d_{3i}$	7.5953	3.0525	0.3000
$d_{4i}$	2.0181	6.5604	9.3287

is inserted to fold the ray path. It is located in front of the first lens, not inside the lens system. Its thickness is just 12 mm, which configuration realizes a much slimmer zoom system. Since the axial rays are parallel to optical axis, there are no aberrations induced by the prism block.

In the initial design, we reduced the aperture and the field size so that the aperture and the image size was too small. If current specifications for a zoom camera are to be met, the aperture and the field size should be increased.

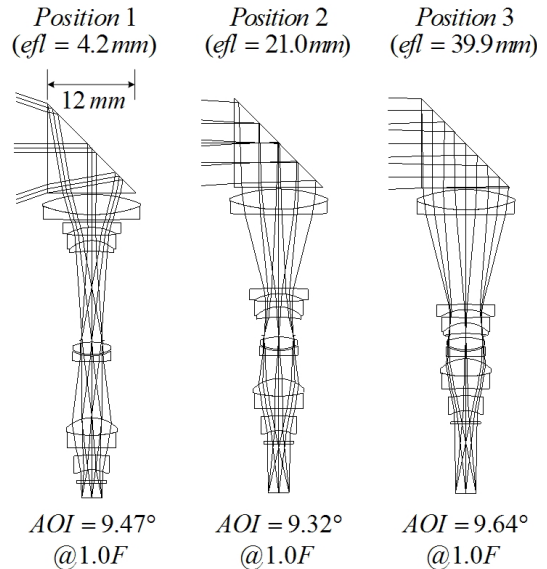


FIG. 13. Layout of an aberration-balanced zoom system having right-angle prism.

The f-numbers are extended to F/3.5 at position 1 and to F/4.5 at position 3. The half image size should be 2.2 mm for 1/4-inch CCD. In an extended aperture and field system, however, higher-order aberrations that are not corrected in the previous design become significant.

In order to improve the overall performance of the zoom system with an extended aperture and field, we balance the aberrations of the starting lens given in Fig. 12 by using the lens design program. In this process, the first-order layouts are fixed. To correct the residual aberrations, we use two aspheric lenses.

The third group relays the refracted ray from the second group to the fourth group. Because the stop is placed in front of the third group, the axial ray heights at that group are very high at all zoom positions. Therefore, the third group generates lots of spherical aberration. Both surfaces of this lens are aspherized to balance the spherical aberrations. The fourth group is designed into a cemented lens and a singlet. To correct the distortion, it will be generally effective to use an aspheric lens at the first group. However, the distortion and the field curvature are corrected by the aspheric surfaces at the last lens of the fourth group in this study. It is, of course, useful to correct these aberrations because the chief ray's height in that lens is high at wide-field position.

Finally, a zoom system having good performance is obtained. The layout of the system is shown in Fig. 13. Table 4 lists the prescription data of the aberration-balanced zoom system. Figure 14 shows the modulation transfer function (MTF) characteristics of the system at two extreme positions. Aberrations are significantly reduced, and the MTF at 200 lp/mm is more than 30% except for marginal fields at all zoom positions. The relative illuminations are calculated at marginal fields for all zoom positions. In this

system, the ratio of relative illuminations is more than 80% over all positions. The chief ray angles of incidence (AOI) into the image plane are shown in Fig. 13. The maximum variation of the AOI from a wide to a narrow field is less than 1.0 degree. That is an extremely small value, so a stable image quality for zooming can be realized. The depth of the zoom lens, even high zoom ratio of 10x, is less than 12 mm, which results in a slim and compact mobile zoom camera. Consequently, this zoom system has enough performance to fulfill the requirements of a current mobile zoom camera.

## V. CONCLUSION

For four-group zoom lens design with high zoom ratio, we set up an inner-focus zoom system consisting of four lens modules with a reduced aperture and field. The optimum initial design with a zoom ratio of 10x was derived

TABLE 4. Final design data of an aberration-balanced zoom system

Surface number	Radius (mm)	Thickness (mm)	Glass code
Object	Infinity	Infinity	
1	Infinity	12.0000	847.238
2	Infinity	0.2000	
3	18.1987	2.7317	703.526
4	-19.6722	0.7000	841.261
5	-164.9049	*0.3000	
6	90.3125	0.7000	793.475
7	6.6565	1.0742	
8	-47.0155	0.7000	816.466
9	4.5000	1.4204	847.238
10	18.8655	*12.0324	
11(stop)	Infinity	0.2000	
12	Ⓐ6.7532	1.6660	560.615
13	Ⓐ-5.5465	0.2000	
14	-5.5203	0.7000	816.466
15	-129.3897	*7.5953	
16	5.0440	2.3577	696.531
17	-13.0579	1.6553	847.238
18	72.1211	0.9579	
19	Ⓐ7.7746	2.0000	816.466
20	Ⓐ3.8456	1.5000	
21	Infinity	0.3000	517.642
22	Infinity	*2.0182	
Image	Infinity	*-0.0090	

(\* denotes the airspaces of moving groups at position 1, and Ⓐ denotes the aspheric surfaces.)

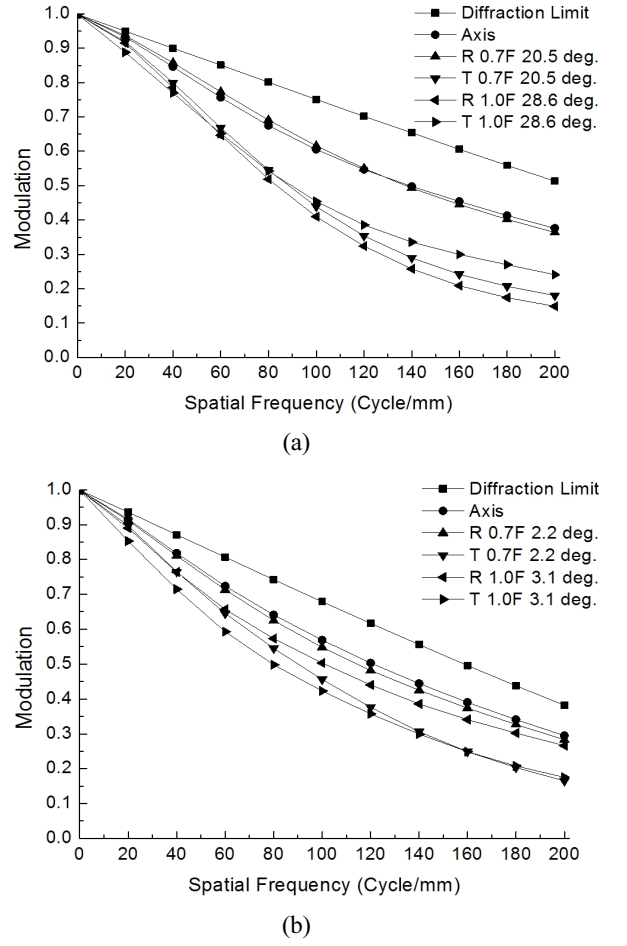


FIG. 14. MTF characteristics of an aberration-balanced zoom system: (a) position 1 and (b) position 3.

by assigning first-order quantities and third-order wave aberrations to each module along with specific constraints. In the lens module zoom system, four lens modules were converted to real lens groups step by step using an automatic design method. From this successive conversion process, the real lens of each group was quickly obtained by matching the four first-order quantities and third-order aberrations of lens modules. This design method is different from previous works in that the past method is to design all groups separately, and then they were combined to establish an actual zoom system.

A prism of 12 mm in thickness was inserted to fold the ray path, which configuration resulted in a slim zoom system having high zoom ratio. Through balancing of the higher-order aberrations in the extended aperture and field, we improved the performance of the zoom system further. A slim zoom system with a zoom ratio of 10x, whose aperture was F/3.5 at wide field and F/4.5 at narrow field, and which had an image size of 1/4-inch on a CCD, was obtained. The zoom system developed in this work performs reasonably as a slim zoom camera with high zoom ratio.

## ACKNOWLEDGMENT

The present research was conducted by the research fund of Dankook University in 2011.

## REREFENCES

1. K. Yamaji, "Design of zoom lens," in *Progress in Optics VI*, E. Wolf ed. (North-Holland, Amsterdam, The Netherlands, 1967), pp. 105-170.
2. M. S. Yeh, S. G. Shiue, and M. H. Lu, "Two-optical-component method for designing zoom system," *Opt. Eng.* **34**, 1826-1833 (1995).
3. K. Tanaka, "Paraxial analysis of mechanically compensated zoom lenses. 1: Four-component types," *Appl. Opt.* **21**, 2174-2183 (1982).
4. K. Tanaka, "Paraxial theory in optical design in terms of Gaussian brackets," in *Process in Optics XXIII*, E. Wolf ed. (North-Holland, Amsterdam, The Netherlands, 1986), pp. 63-111.
5. J. H. Lee, T. S. Jang, H. S. Yang, and S. W. Rhee, "Optical design of a compact imaging spectrometer for STSAT3," *J. Opt. Soc. Korea* **12**, 262-268 (2008).
6. O. Stavroudis and R. Mercado, "Canonical properties of optical design modules," *J. Opt. Soc. Am.* **65**, 509-517 (1975).
7. T. G. Kuper and M. P. Rimmer, "Lens modules in optical design," *Proc. SPIE* **892**, 140-151 (1988).
8. S. C. Park and Y. J. Jo, "Ultra-slim zoom lens design for a 3x mobile camera," *J. Korean Phys. Soc.* **52**, 1048-1056 (2008).
9. S. C. Park, Y. J. Jo, B. T. You, and S. H. Lee, "Optical zoom system design for compact digital camera," *J. Korean Phys. Soc.* **50**, 1243-1251 (2007).
10. S. C. Park and R. R. Shannon, "Zoom lens design using lens module," *Opt. Eng.* **35**, 1668-1676 (1996).
11. S. C. Park, S. H. Lee, and J. G. Kim, "Compact zoom lens design for a 5x mobile camera using prism," *J. Opt. Soc. Korea* **13**, 206-212 (2009).
12. M. T. Chang, *Pupil Aberration in Modular Zoom Lens Design*, Ph.D. dissertation paper, University of Arizona, AZ, USA (1998).
13. W. T. Welford, *Aberration of Optical Systems* (Adams Hilger Ltd., Bristol, UK, 1986), Chapter 8.
14. M. Herzberger, *Modern Geometrical Optics* (Interscience, New York, USA, 1958).
15. W. J. Smith, *Modern Optical Engineering: The design of Optical Systems* (McGraw-Hill, New York, USA, 1990).
16. Masafumi Sueyoshi, U. S. Patent 7110186 (2006).
17. CODE V Reference Manual, Version 9.70 (Optical Research Associations, Pasadena, CA, USA, 2007).